Organic Geochemistry 138 (2019) 103924

Contents lists available at ScienceDirect

Organic Geochemistry

journal homepage: www.elsevier.com/locate/orggeochem

Group I alkenones and Isochrysidales in the world's largest maar lakes and their potential paleoclimate applications

Karen J. Wang [a,*], Jonathan A. O'Donnell [b], William M. Longo [c], Linda Amaral-Zettler [a,d,e], Gaoyuan Li [f], Yuan Yao [a,g], Yongsong Huang [a,g,*]

[a] Department of Earth, Environmental and Planetary Sciences, Brown University, Providence, RI 02912, USA
[b] Arctic Network, National Park Service, Anchorage, AK, USA
[c] Department of Marine Chemistry and Geochemistry, Woods Hole Oceanographic Institution, Woods Hole, MA 02543, USA
[d] Department of Marine Microbiology and Biogeochemistry, NIOZ Royal Netherlands Institute for Sea Research and Utrecht University, the Netherlands
[e] Department of Freshwater and Marine Ecology, Institute for Biodiversity and Ecosystem Dynamics, University of Amsterdam, the Netherlands
[f] State Key Laboratory of Biogeology and Environmental Geology, China University of Geosciences, Beijing 100083, China
[g] State Key Laboratory of Loess and Quaternary Geology, Institute of Earth Environment, Chinese Academy of Sciences, Xi'an 710061, China

ARTICLE INFO

Article history:
Received 17 May 2019
Received in revised form 6 August 2019
Accepted 30 August 2019
Available online 31 August 2019

Keywords:
Alkenones
Isochrysidales
Espenberg maar lakes
Seward Peninsula
Alaska
AgTCM
18S rRNA
Paleotemperature

ABSTRACT

The Espenberg maar lakes on the Seward Peninsula, Alaska, are the largest volcanic crater lakes in the world and contain the longest known lacustrine sedimentary archives in Alaska. The lack of glacial-aged marine sedimentary archives around the Bering Land Bridge due to exposure of the shelf during sea level low-stands makes these lakes highly valuable for understanding the region's past climate and environmental changes. Located en route to humanity's last colonized American continents, the Seward Peninsula's climate and environments during the last glacial period bear major anthropological significance. However, a lack of quantitative proxies has so far hampered exploration of these lakes for paleoclimate reconstructions. Here we report, for the first time, the discovery of abundant Group I alkenones and Isochrysidales in surface sediments from three maar lakes: White Fish, North Killeak and Devil Mountain, using a combination of lipid biomarker and 18S rRNA gene sequencing analyses. Our discovery adds to the expanding list of oligotrophic freshwater lakes where Group I alkenones are found, and water chemistry data contribute to the understanding of the environmental controls on Group I Isochrysidales. Our results further confirm the use of the U^{K}_{37} index of Group I alkenones as a proxy for the mean temperature of the spring isotherm (MTSI) and RIK_{37} as a quantitative measurement for Isochrysidales group mixing. We also demonstrate the analytical challenges for analyzing alkenones in freshwater lakes and the effectiveness of eliminating coelution using silver thiolate chromatographic material (AgTCM).

© 2019 Elsevier Ltd. All rights reserved.

1. Introduction

East Beringia is important for climatology, ecology, and anthropology (Chapin et al., 2014; Hugelius et al., 2014; Vachula et al., 2019). The regional temperature has been rising twice as fast as the global average over the last 50 years (Chapin et al., 2014), and is ecologically and climatically important with its vast tundra ecosystems underlain by carbon-rich permafrost soils (Hugelius et al., 2014). The large carbon reservoir stored in tundra soils has the potential to exert a major feedback to the climate system upon thawing and subsequent carbon release to the atmosphere if the temperature continues to rise rapidly (Schuur et al., 2015). Research in this region is also critical for understanding the final migration of modern humans from East Asia to the Americas during the last glacial period. The model and timing of human migration to Alaska are widely debated: with one hypothesis suggesting a "swift peopling" at ca. 14,000 years ago prior to the submergence of the Bering Land Bridge by the rising sea level (Gilbert et al., 2008; Goebel et al., 2008), and the other so-called "Beringian Standstill Hypothesis (BSH)" proposing a much earlier migration during the last glacial period. The BSH theorizes, based on population genetics, that Native American ancestors once inhabited east Beringia for over 10,000 years around or prior to the Last Glacial Maximum (LGM, ~21,000 years ago), before rapidly colonizing the Americas as the Laurentide Ice Sheet (LIS) retreated during the deglaciation (Tamm et al., 2007; Hoffecker et al., 2016; Moreno-Mayar et al., 2018). A recent study of fecal biomarkers

* Corresponding authors at: Department of Earth, Environmental and Planetary Sciences, Brown University, Providence, RI 02912, USA (Y. Huang, K.J. Wang).
E-mail addresses: karen_wang@brown.edu (K.J. Wang), yongsong_huang@brown.edu (Y. Huang).

https://doi.org/10.1016/j.orggeochem.2019.103924
0146-6380/© 2019 Elsevier Ltd. All rights reserved.

and biomass burning from northern Alaska supports the BSH and provides new evidence of human settlement in the region at ~32,000 years ago (Vachula et al., 2019). Modeling studies suggest regional temperatures could have been particularly warm in comparison to other Arctic regions during the LGM, due to the potentially high elevation and topography of the LIS blocking and deflecting warm air of subtropical origin to northern Alaska (Bartlein et al., 2011; Brady et al., 2013). As a result, ancient east Beringians living in Alaska would have benefitted from conditions that were substantially warmer than on the Siberian side of Beringia (i.e., west Beringia).

The important scientific problems detailed above cannot be fully addressed until long quantitative temperature reconstructions are obtained from east Beringia. Unfortunately, interpretations of the common measurable oceanographic proxies in this region are complicated by the great stratigraphic variability due to marine transgressions and influences of different water masses and freshwater input on the foraminifera isotopic composition (Knebel et al., 1974; Miller et al., 2010). Thus, lakes that hold long terrestrial sedimentary records extending to last glacial maximum and beyond are highly valuable for paleoclimate reconstructions. Espenberg maar lakes on the Seward Peninsula, Alaska, are of particular significance in this regard, as they were formed by phreatomagmatic eruptions between 7100 years to up to 200,000 years ago and are the world's largest crater lake complexes (Hopkins, 1988; Begét et al., 1996). Traditional paleolimnological proxies applied in lakes encounter major challenges and complications in this region: e.g., the non-analog pollen assemblages during the LGM (Bartlein et al., 2011), and chironomid assemblages potentially affected by water depth and other lake specific effects related to re-deposition and transport processes (Kurek and Cwynar, 2009). Therefore, discovering a new proxy for reconstructing past temperatures from the Espenberg maar lakes bears major paleoclimatic, paleoceanographic and anthropological significance.

We report here an initial study of lake surface sediments from three Espenberg maar lakes (White Fish, North Killeak, and Devil Mountain) and the discovery of Group I alkenones and their producers, Group I Isochrysidales, using combined organic geochemical and environmental DNA-based phylogenetic approaches. The Group I alkenones were first discovered in southwestern Greenland (D'Andrea and Huang, 2005; D'Andrea et al., 2006). Subsequent systematic comparison of 18S rRNA gene sequences has grouped Isochrysidales, an order of haptophyte algae known to produce alkenones, into three different groups, with freshwater species being Group I, open ocean species (*Emiliania huxleyi* and *Gephyrocapsa oceanica*) as Group III, and other coastal or saline lake species (e.g., *Ruttnera lamellosa*, *Isochrysis galbana*, *Tisochrysis lutea*) as Group II (Theroux et al., 2010). Alkenones produced by Group I Isochrysidales bear distinct molecular distributions with a high abundance of the $C_{37:4}$ alkenone and the presence of a set of $C_{37:3}$ double bond positional isomers, which are readily resolved using a mid-polarity gas chromatography column (Longo et al., 2013; Zheng et al., 2017). Water column particulate matter and a survey of surface sediments from lakes in the Northern Hemisphere have yielded a water temperature calibration (D'Andrea et al., 2011; Longo et al., 2016), as well as air temperature calibrations (Longo et al., 2018). Particularly, Group I Isochrysidales bloom in early spring (D'Andrea et al., 2011; Longo et al., 2016), and have been shown to record cold season air temperatures through Group I alkenones (Longo et al., 2018), which is in contrast with the majority of geochemical proxies which record warm growth season temperatures. We compare our data with previous U^K_{37} temperature calibrations and discuss the potential applications of alkenones in Espenberg maar lakes for paleoclimate reconstructions.

2. Material and methods

2.1. Regional settings

The studied lakes are situated in the Devil Mountain–Cape Espenberg volcanic field, which is a segment of the northern coastal plain of the Seward Peninsula, Alaska, in the National Park Service's (NPS) Bering Land Bridge National Preserve. The maar lakes are the largest volcanic crater lakes in the world and were formed by phreatomagmatic eruptions when rising basaltic magma encountered groundwater in Cenozoic sediments beneath hundreds of meters of ice-rich permafrost (Begét et al., 1996). The three maar lakes, Devil Mountain Lake, North Killeak Lake and White Fish Lake (Fig. 1), where we collected surface sediments, were formed during different eruptions. The estimated age based on tephra deposition is 7100 years for Devil Mountain Lake, >125,000 years for North Killeak Lake and 100,000–200,000 years for White Fish Lake (Hopkins, 1988; Begét et al., 1996).

The surface areas of White Fish Lake (7.68 km^2) and North Killeak Lake (9.17 km^2) are similar in size, while Devil Mountain Lake, the biggest maar lake on Earth, has a surface area of 21.23 km^2. White Fish Lake has a maximum depth of around 6 m and contains organic-rich, diatomaceous sediment, North Killeak Lake is about 25 m deep, and Devil Mountain Lake is >100 m deep with a more complex bathymetry surrounded by pyroclastic rocks (Begét et al., 1996).

2.2. Climate data

We retrieved climate data following the procedures described by Longo et al. (2018). Data were downloaded from the WorldClim Global Climate Database (worldclim.org; Hijmans et al., 2005) using the Senckenberg data extraction tool (dataportal-senckenberg.de/dataExtractTool). WorldClim 1.4 data were derived from monthly air temperature and precipitation data compiled from globally distributed weather stations by the Global Historical Climatology Network, the World Meteorological Organization, the Food and Agriculture Organization of the United Nations, and others (Hijmans et al., 2005). The high-resolution interpolated climate products for current condition are only available for year 1950–2000. We therefore used these temperatures for our calibration study. Mean monthly temperatures (1950–2000) of the sites from Worldclim climatology data are shown in Supplementary Fig. S1.

Mean annual air temperature (MAAT), mean temperature of the warmest quarter (MTWQ) and mean temperature of the spring isothermal season (MTSI) were calculated by temperature regression of the samples from this study and its comparison between the compilation of Northern Hemisphere dataset from Longo et al. (2018). Since the sedimentation rates of the lakes in this study are unknown, the surface sediments are assumed to represent the average temperature in the past few decades, monthly mean from 1950 to 2000 climate data were used in calculations and regressions.

2.3. Sample collection

The study lakes are remote and pristine with no road access, and sample collection was carried out with aviation support from the Arctic Inventory and Monitoring Network (ARCN) program of the National Park Service. Samples and measurements were taken from Cessna 185F floatplane landing directly onto the sampling lakes in September 2017. After water depth measurement, surface sediments were collected using an Ekman dredge, wherein approximately 100 g of sediment was separated from the top ~5 to 10 cm

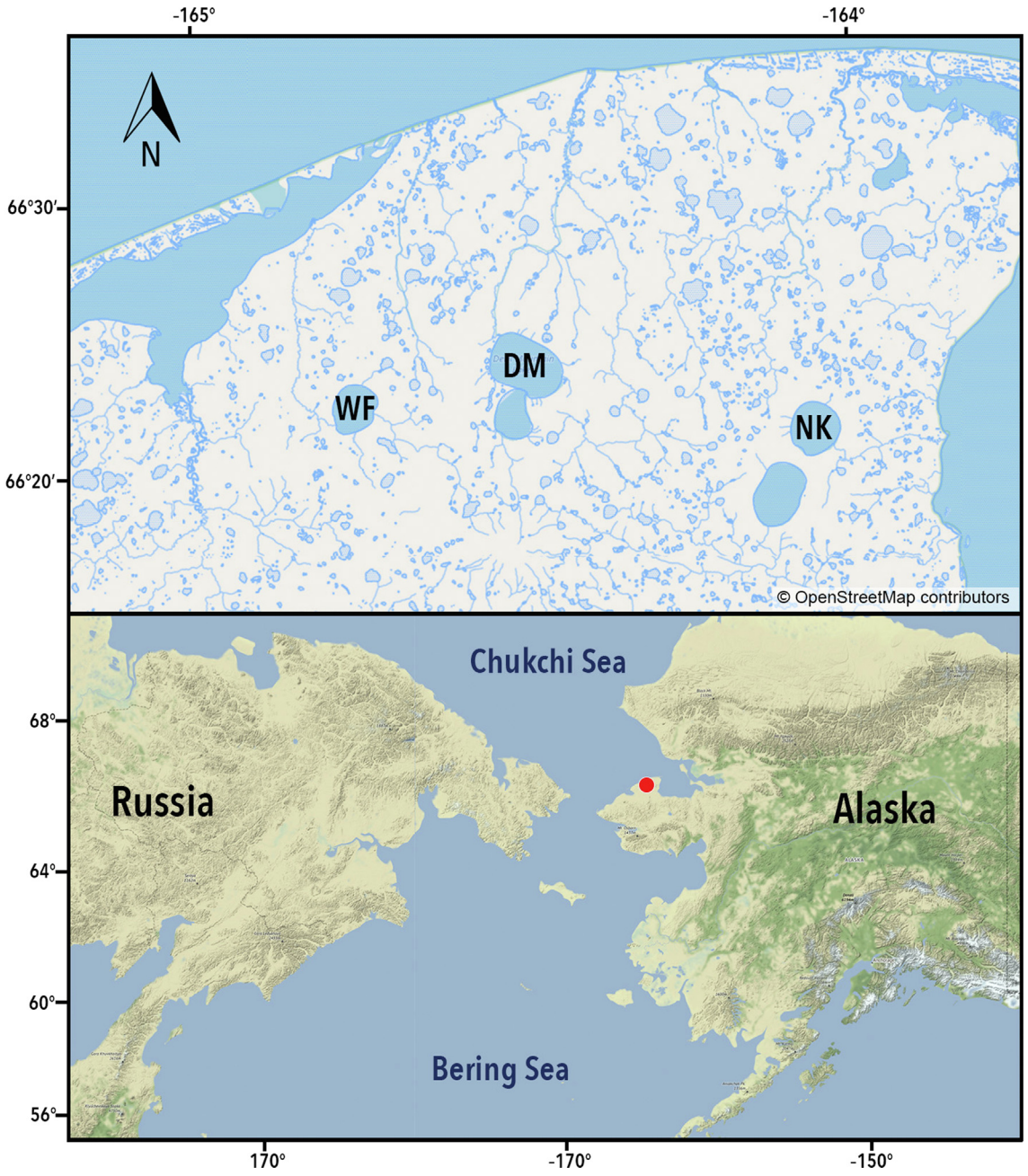


Fig. 1. Maps of the study region and the hydrology of sampled sites. WF: White Fish Maar, DM: Devil Mountain Maar, NK: North Killeak Maar.

of each sediment grab using sterile scoops and transferred into whirl-pak sampling bags for later DNA analysis. One surface sediment sample from Toolik Lake (68°38′N, 149°36′W), northern Alaska, collected previously (Longo et al., 2016) and kept frozen at −20 °C, was also studied for comparison with the maar lakes. Water column and surface sediment samples from Toolik Lake have previously been found to contain Group I alkenones and Isochrysidales (Richter et al., 2019). The specific sampling locations for the three lakes are: White Fish (66°22′N, 164°45′W; water depth = 2.2 m), North Killeak (66°21′N, 164°20′W; water depth = ~3 m) and Devil Mountain (66°24′N, 164°29′W; water depth = ~6 m). One surface sediment sample was taken from each lake for alkenone and phylogenetic analyses, with the assumption that these samples were representative of the alkenone profiles and genetic diversity of the individual lakes. Samples were frozen until DNA extraction.

Lake surface water samples were collected for chemical analyses as part of the National Park Service's ARCN lake monitoring program (O'Donnell et al., 2015). Chemistry data are reported in Supplementary Table S2 and represent the average (±one standard deviation) of two to three sampling dates (6/22/2013, 7/15/2015, and 9/15/2017). Water samples were collected at 0.5 m below the lake surface in the pelagic zone using a 0.45 µm high-capacity capsule filter connected to a Geopump Series II Peristaltic Pump (Geotech Environmental Equipment Inc., Denver, CO). DOC concentrations were determined using an O.I. Analytical Model 700 TOC analyzer via the platinum catalyzed persulfate wet oxidation method (Aiken, 1992). UV-visible absorbance was measured on filtered stream samples at room temperature using a quartz cell with a path length of 1 cm on an Agilent Model 8453 photodiode array spectrophotometer. Specific UV absorbance at 254 nm ($SUVA_{254}$) was determined for all stream samples by dividing the

decadal UV-visible absorbance coefficient at λ = 254 nm by DOC concentration. $SUVA_{254}$ (L mg C^{-1} m^{-1}), which is typically used as an index of DOC aromaticity, provides an average absorptivity at λ = 254 nm of the dissolved organic matter (DOM; Weishaar et al., 2003). To determine DIC concentrations, stream water samples were collected without head space in a 60 mL syringe. Immediately prior to analysis, water samples were filtered using 0.45 μm nylon syringe filters into 40 mL borosilicate clean vials and capped by septum caps to minimize interaction with the atmosphere. DIC concentrations were determined by acidifying with phosphoric acid and measuring on a Shimadzu TOC-VCSH Combustion Analyzer. Base cation concentrations (Ca^{2+}, Mg^{2+}, Na^{+}, K^{+}) were determined on a Shimadzu AA-7000 atomic absorption spectrophotometer, and major anions (Cl^{-}, SO_4^{2-}) were determined on a Dionex 1500 ion chromatograph. Alkalinity was determined via titration using a ManTech PC-Titrate auto titrator system. Total dissolved nitrogen was determined by persulfate digestion on a Technicon Auto-Analyzer II. pH was measured in situ using a YSI multi-parameter probe.

2.4. Alkenones analysis

Surface sediment samples were freeze-dried. Around 10 g of freeze-dried sediment were extracted by Dionex™ accelerated solvent extraction (ASE) system with dichloromethane (DCM):methanol mixture (9:1, v/v). The total lipid extract was separated into alkane, ketone and polar fractions by silica gel columns based on different polarity using the following eluents: hexane, DCM, and methanol. The ketone fractions that contain the alkenones and esters were saponified in 1 M KOH in methanol:H_2O (95:5, v/v) solution and heated at 65 °C for 3 h. The resulting products were acidified to pH <2 by adding drops of 3 M HCl, followed by hexane extraction, and purified by silica gel columns. The alkenones were further purified using silver thiolate silica gel columns (AgTCM; Aponte et al., 2013; Wang et al., 2019) before analysis by gas chromatography-flame ionization detection (GC-FID) using a mid-polarity GC column VF-200 ms (Zheng et al., 2017).

2.5. DNA extraction and analysis

Genomic DNA was extracted from ~500 mg surface sediments and purified using FastDNA™ SPIN Kit for Soil (MP Biomedicals, OH, USA) and DNeasy PowerClean Pro Cleanup Kit (Qiagen, Carlsbad, CA, USA) according to the manufacturer's instructions. The V4 18S rRNA coding region was amplified using Prym-429F and Prym-887R (Coolen et al., 2004), and modified PCR conditions optimized for this sample set: denaturing 4 min at 96 °C, followed by 35 cycles including denaturing (30 s at 94 °C), 40 s of primer annealing at 61.5 °C, and primer extension (40 s at 72 °C). A final extension was performed at 72 °C (10 min). Each sample was run at three different dilutions (1:10, 1:100, 1:1000) to achieve maximum product yield, with a positive control, a negative control and an extraction blank included in each run. The PCR products were examined by gel electrophoresis and purified with the AxyPrep DNA Gel Extraction Kit (Axygen, USA). Cloning using the pGM-T Cloning Kit (Tiangen Biotech, Beijing, China) and Sanger sequencing on an ABI 3730XL capillary sequencer (Applied Biosystems, Foster City, CA) were performed by Shanghai Majorbio BioPharm Technology Co., Ltd., China (www.majorbio.com). Only sequences longer than 400 bp with complete forward and reverse primer intact were retained. Sequences are deposited in GenBank under accession numbers MK208448–MK208452.

The raw capillary sequence data yielded 146 haptophyte sequences after Chimera checking with ChimeraSlayer (Haas et al., 2011). Operational Taxonomic Units (OTUs) were clustered using UCLUST with a 97% cut-off criterion (Edgar, 2010). Representative sequences were picked for each OTU in QIIME/1.9.1 (Caporaso et al., 2010). Closest relatives of the OTUs were identified through BLAST queries against NCBI GenBank database. Representative sequences were then aligned against a curated alignment from Gran-Stadniczeñko et al. (2017) using PyNast (Caporaso et al., 2009). The alignment and selected outgroup *Prymnesium faveolatum* (ALGO HAP79) were used to infer a phylogeny using the Randomized Axelerated Maximum (RAxML) program (Huelsenbeck and Crandall,1997; Stamatakis, 2014). Rapid bootstrapping with 1000 bootstrap replicates and an ML search under the GAMMA model of rate heterogeneity were conducted.

3. Results

3.1. Phylogenetic analysis

Isochrysidales sequences (116 in total) were recovered from the clone libraries and analyzed, including 26 from White Fish Lake, 9 from Devil Mountain Lake, 60 from North Killeak Lake, and 21 from Toolik Lake. The sequences were clustered into five OTUs, namely Alaska OTU 0–4, among which Alaska OTU0 constitutes all the sequences from White Fish Lake, Devil Mountain Lake, Toolik Lake and the majority of sequences from North Killeak Lake. The other four OTUs only include sequences from North Killeak Lake and included 1–3 Isochrysidales sequences recovered in each OTU (Table 1).

The phylogenetic tree shows that Isochrysidales sequences are clustered into three groups, with Groups I and III Isochrysidales forming a sister clade to Group II Isochrysidales (Fig. 2), consistent with the new phylogenic analyses showing common ancestry of Group I and III Isochrysidales (Richter et al., 2019). Alaska OTUs 0, 1, 2 and 4 were all identified as Group I Isochrysidales, with branch lengths relatively long compared to the branch lengths within Group II and Group III Isochrysidales. OTU 0 showed robust branching with the uncultured haptophyte from BrayaSø, Greenland (HQ446254, Fig. 2). Alaska OTU 3 fell into Group II and is closely related to *Isochrysis galbana*. The occurrence of Group II is very uncommon in the low salinity (1.1 ppt) environment of North Killeak.

3.2. Alkenone profiles and proxy indices

Alkenones were found in the surface sediments of all three lakes. Saponification and AgTCM columns were processed sequentially in order to separate the co-eluting compounds. Saponification successfully removed the co-eluting wax esters. AgTCM columns were applied to further remove other non-ester compounds that were co-eluting mainly with $C_{37:2Me}$, $C_{38:3aEt}$, and $C_{38:4Me}$. This method can efficiently separate all alkenones from co-eluting impurities such as steryl ethers and various saturated ketones with variable carbonyl positions (Supplementary Fig. S2; Wang et al., 2019). The final alkenone profiles after cleanup steps demonstrate clear Group I-type distributions including dominant $C_{37:4}$ and $C_{37:3}$ isomers, and the presence of C_{38Me} alkenones (Fig. 3). The results suggest it is important to remove coeluting compounds from alkenones using AgTCM columns (or other approaches) for accurate alkenone analysis.

The alkenone peaks are well resolved for accurate quantification after the saponification step and AgTCM column separation. Alkenone concentrations and U^{K}_{37}, $U^{K'}_{37}$, $\%C_{37:4}$, and RIK_{37} values are shown in Supplementary Table S1, as well as the MAAT, MTWQ, and MTSI values of the three lakes. Calibrations between $U^{K}_{37}$and temperatures were calculated using data from this study and data from lakes distributed throughout the mid- and high-latitudes of the Northern Hemisphere compiled by Longo et al.

Table 1
Summary of the sequences recovered from each sample, and their phylogenetic assignments.

Sample	Numbers of Isochrysidales sequences recovered from clone libraries					
	Total	Group I				Group II
		OTU 0	OTU 1	OTU 2	OTU 4	OTU 3
White Fish	26	26	0	0	0	0
Devil Mountain	9	9	0	0	0	0
North Killeak	60	52	2	1	3	2
Toolik	21	21	0	0	0	0

(2018). U^K_{37} values yield a positive correlation with MAAT, MTWQ, and MTSI (Fig. 4). Though the correlations between U^K_{37} and MAAT ($U^K_{37} = 0.007 \times T - 0.4746$, $R^2 = 0.25$, $p = 9.9e{-}3$), MTWQ ($U^K_{37} = 0.0011 \times T - 0.6206$, $R^2 = 0.31$, $p = 3.4e{-}3$) are weak, they showed significant correlation between U^K_{37} and MTSI ($U^K_{37} = 0.031 \times T - 0.4858$, $R^2 = 0.59$, $p = 4.0e{-}6$).

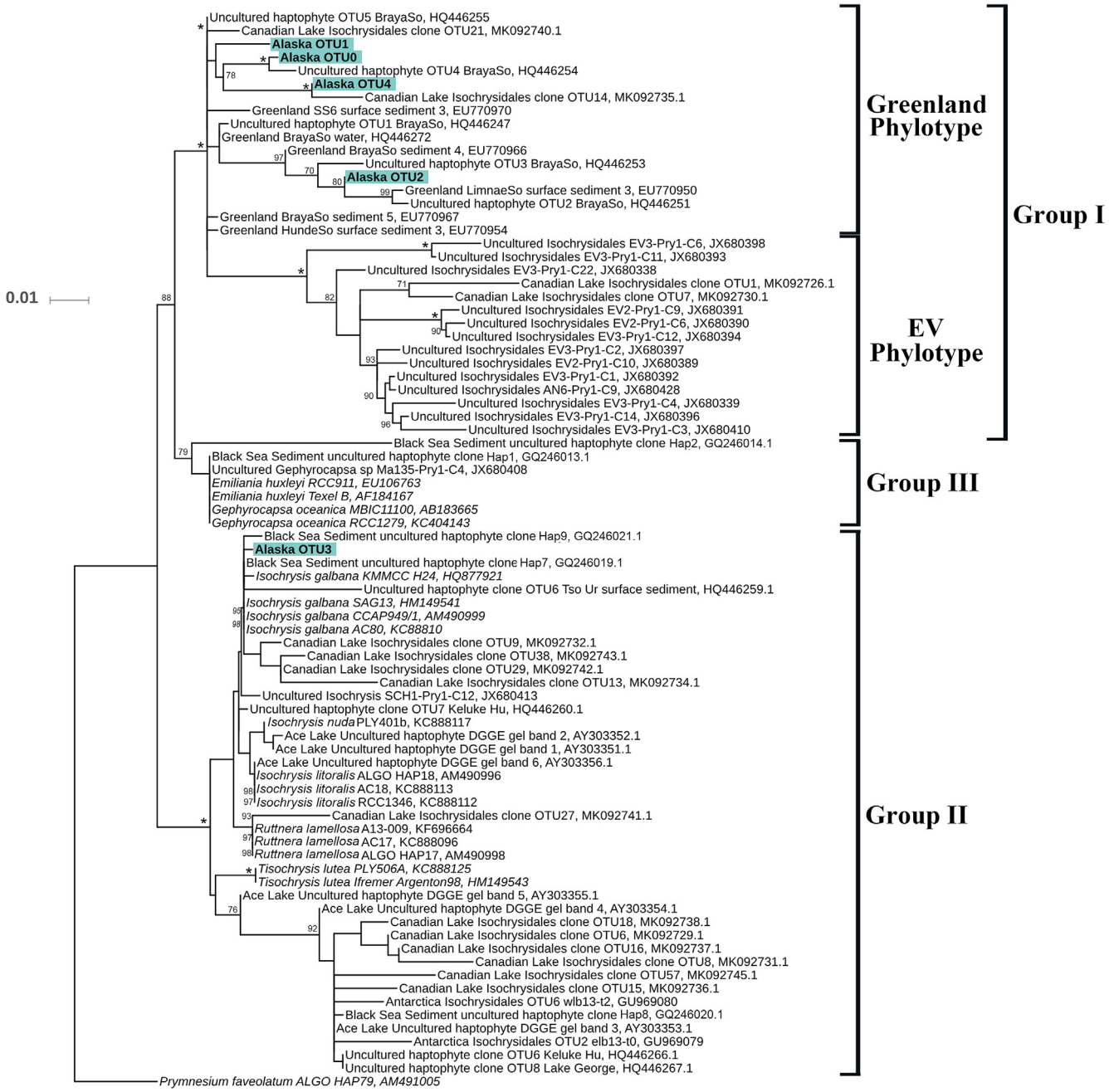


Fig. 2. Maximum likelihood tree showing the phylogeny of Isochrysidales constructed from partial 18S rRNA gene sequences. Sequences recovered from this study (Alaska OTU 0–4) are in bold with GenBank number following. Groups I, II and III Isochrysidales clades are labeled after Theroux et al. (2010), Greenland phylotypes include the sequence recovered in Greenland freshwater lakes from D'Andrea et al. (2006) and four OTUs from this study, and EV phylotypes include sequences from Simon et al. (2013). Only bootstrap values > 70% are shown, asterisks represent bootstrap values equal to 100%.

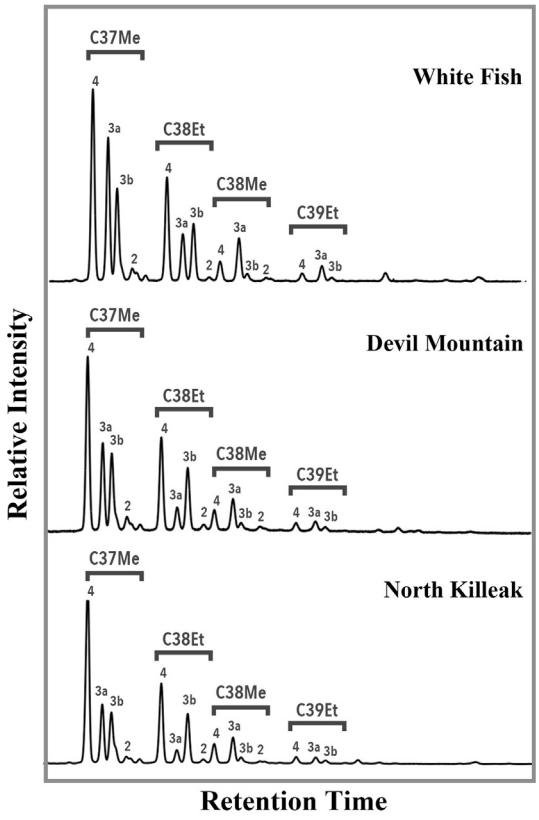


Fig. 3. Partial chromatograms of the surface sediments from the three studied maar lakes after saponification and AgTCM column. The alkenones showed distinctive Group I characteristics.

4. Discussion

4.1. Water chemistry and the occurrence of Group I Isochrysidales

Freshwater or oligohaline conditions with relatively high pH and alkalinity have been proposed to be the key environmental factors that allow Group I Isochrysidales to thrive (Longo et al., 2016). However, not all fresh/oligohaline lakes with elevated pH host Group I Isochrysidales. Despite previous investigations including water chemistry of lakes hosting Group I Isochrysidales (e.g., Longo et al., 2018; Plancq et al., 2018a), the environmental controls are not fully known. Fortunately, the ARCN program has water chemistry monitoring data for our studied lakes, providing another opportunity to explore this topic (Supplementary Table S2).

The maar lakes in this study are characterized by an elevated pH of 8.3–8.4, with values comparable to shallow lakes where the drainage basins are underlain by volcanic deposits in the region (Larsen et al., 2017), but are higher than those reported in freshwater lakes north of the Brooks Range, Alaska, which also contain Group I Isochrysidales and corresponding alkenones (pH 6.2–8.5; Longo et al., 2016). Alkalinity of the maar lakes is comparable to the northern Alaskan lakes (Supplementary Table S2; Longo et al., 2016), but significantly higher than those reported from other non-maar lakes in the Toolik region of Alaska (~0 mg$CaCO_3$/L; Luecke et al., 2014) and Russia (0–0.05 mg$CaCO_3$/L; Drake et al., 2019). The dominant cations are Na^+, Mg^{2+}, and Ca^{2+} (Supplementary Table S2). These characteristics indicate the relatively fast rate of weathering from tephra and basalt containing a high abundance of mafic minerals such as olivine, pyroxene, and plagioclase (Pecoraino et al., 2015): $CO_2 + H_2O$ + sodium-rich tephra and volcanic glass + basalt (plagioclase $NaAlSi_3O_8 + CaAl_2Si_2O_8$; olivine $(Mg, Fe)_2SiO_4$; pyroxene $XY(Si,Al)_2O_6$) → clay minerals + $Ca^{2+} + Mg^{2+} + Na^+ + HCO_3^-$

Ca^{2+} and Mg^{2+} concentrations in the maar lakes are similar to streams and rivers draining in the nearby terrain (O'Donnell et al., 2015, 2016), suggesting weathering reactions primarily take place in the surrounding soils that overlay tephra, volcanic glass, and basalt. High-purity igneous rocks are composed of silicate minerals almost devoid of anionic components such as Cl^-. Thus the high Cl^- and associated Na^+ indicate that the nearby Bering Sea exerts a strong marine influence on lake chemistry of the Seward Peninsula during the open-water period (June–September; Larsen et al., 2017), as evidenced by the relatively high concentrations of Na^+ and Cl^- in White Fish Lake and North Killeak Lake in comparison to Devil Mountain Lake which is farther away from the coastline.

Environmental sulfur has been suggested as an essential element for all photosynthetic algae (Takahashi et al., 2011; Giordano and Prioretti, 2015; Plancq et al., 2018a), and Group I Isochrysidales have been detected in Canadian Prairies lakes with elevated sulfate content (93.4–1878 mg/L; Plancq et al., 2018a). However, in contrast to the Canadian Prairies lakes (Plancq et al., 2018a) and similar to the northern Alaskan lakes (Longo et al., 2016), the three maar lakes in this study all have very low sulfate concentrations, extending the lower limit of sulfate concentrations observed for Group I Isochrysidales. Some interesting spatial differences in carbon and nutrient concentration across maar lake basins have been observed. At North Killeak and Devil Mountain Lakes, dissolved inorganic nitrogen species (nitrate, ammonium) were below the detection limit, and phosphate concentrations were very low. Organic nutrient species (as reflected by total N and P, and total dissolved N and P) concentrations were also low at North Killeak and Devil Mountain Lakes. These highly oligotrophic conditions are common in lakes of Arctic Alaska (Luecke et al., 2014; Larsen et al., 2017). However, concentrations of organic and inorganic N and P species were substantially higher at White Fish compared to the other maar lakes in this study. Further, DOC concentration and $SUVA_{254}$, which serves as an index of DOM aromaticity (Weishaar et al., 2003), are highest in White Fish Lake compared with other large lakes (N = 20) surveyed in three Arctic parks as part of the NPS ARCN lake monitoring program (O'Donnell et al., 2015). Terrestrial DOM may serve as an important source of nutrients to phytoplankton in White Fish Lake, driving high rates of primary productivity in the lake. Alternately, high concentrations of DOC may originate from the decomposition of particulate carbon or algal exudate in the water column. Repeated cyanobacteria blooms were observed in White Fish Lake during a July 2018 site visit, and the organic-rich sediments collected by Ekman dredge indicate that White Fish Lake is mesotrophic.

In summary, the elevated pH, alkalinity, and low salinity of the Espenberg maar lakes are similar to the lakes hosting Group I Isochrysidales in Greenland (D'Andrea et al., 2006; Theroux et al., 2010), northern Alaska (Longo et al., 2016), Canadian Prairies (Plancq et al., 2018a), and northeastern China (Yao et al., personal communication). However, the occurrence of Group I Isochrysidales in the mesotrophic White Fish Lake expands our previous understanding of the environmental preference of Group I Isochrysidales which have mostly been found in oligotrophic lakes.

4.2. Genetic variation within Group I and II Isochrysidales

Longo et al. (2016) found freshwater lakes from northern Alaska featured distinct distributions of Group I alkenones. Their analysis of suspended particulate matter (SPM) from Toolik Lake yielded

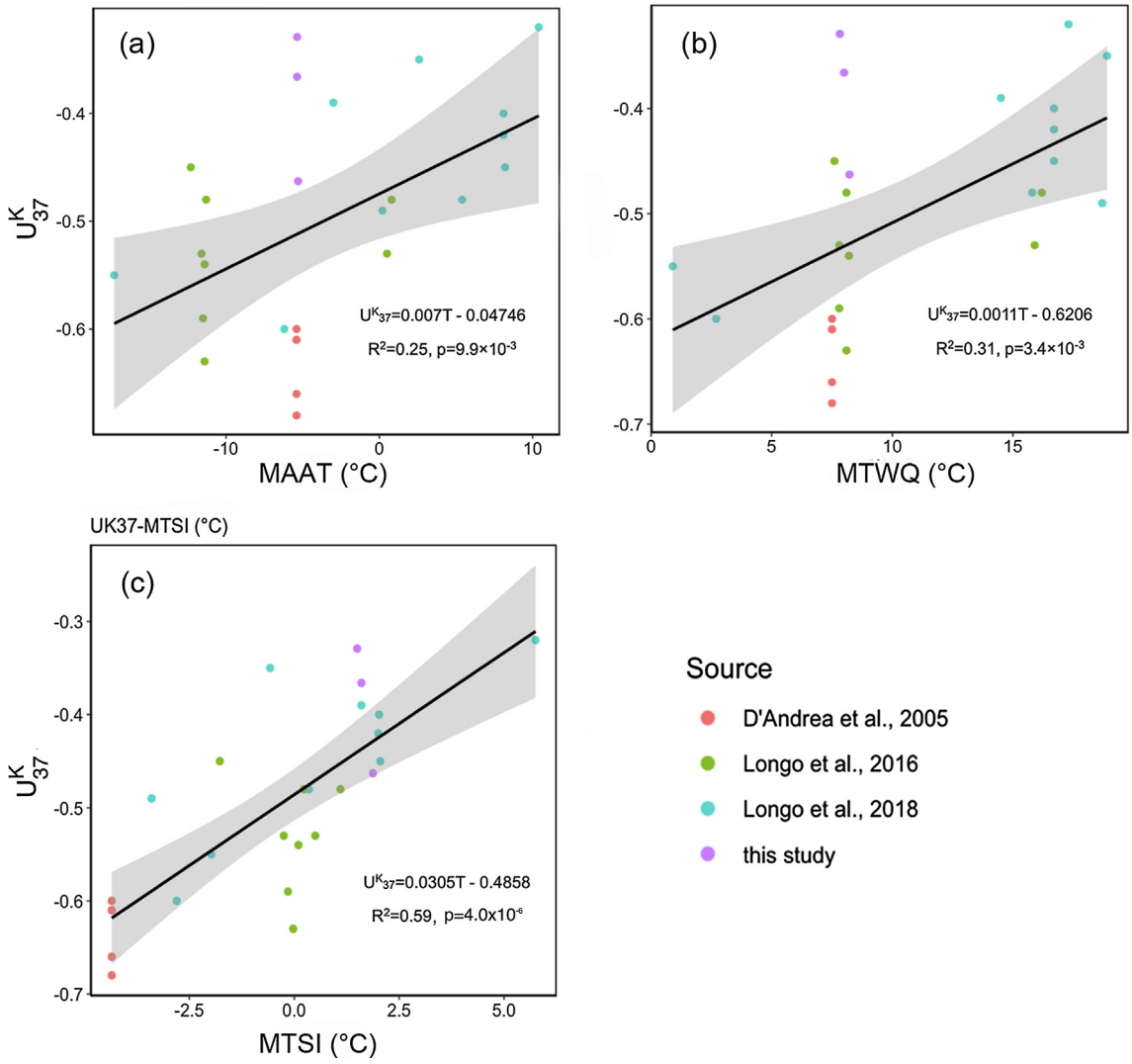


Fig. 4. Regressions between U^K_{37} and mean annual air temperature (MAAT, a), mean temperature of the warmest quarter (MTWQ, b), and mean temperature of the spring isotherm (MTSI, c). Shaded areas represent 95% confidence interval.

the first in situ freshwater U^K_{37} calibration. Previous studies have examined the alkenone producers in Toolik lakes using primers targeting the eukaryotic V9 hypervariable region of the small-subunit (SSU) rRNA gene and haptophyte V4 SSU rRNA gene from water samples, showing that the alkenone producers in Toolik Lake during the sampling season belong to Group I Isochrysidales (Crump et al., 2012; Richter et al., 2019). In this study, we extracted DNA from surface sediments and applied pre-existing haptophyte-specific V4 SSU rRNA gene primers (Coolen et al., 2004). The molecular data confirmed the common presence of Group I Isochrysidales DNA in sediments and showed that the alkenone producers in Espenberg maars and Toolik Lake are highly similar.

The most abundant Isochrysidales OTU in this study is Alaska OTU 0 that constituted all the sequences recovered from White Fish, Devil Mountain, and Toolik Lakes, and the majority of the sequence recovered from North Killeak Lake. Alaska OTU 0 is closely related to the uncultured haptophyte (HQ446254) from BrayaSø, West Greenland. OTU 1, 2, and 4 show branching among other Group I sequences from Greenland and Canadian Prairies. Those sequences grouped with Greenland phylotypes separate from a clade that consists of sequences recovered from lake Etang des Valles, France (EV phylotypes). Due to primer mismatches, the primer pair we used in this study cannot detect EV phylotypes (Richter et al., 2019). Therefore, it is possible that we did not recover the full Group I Isochrysidales genetic diversity present in these maar lakes. However, since the EV phylotypes are of low abundance in Toolik lake based on high-throughput sequencing data (Richter et al., 2019), and the most abundant OTU in this study branches with a Greenland phylotype with strong support, it is possible that alkenones in Toolik Lake, Alaska maar lakes and BrayaSø have similar temperature sensitivities.

There are still some lingering questions regarding the genetic diversity observed in the current data. North Killeak Lake contains all the OTUs recovered in this study, while the other lakes only contain OTU 0. Notably, Alaska OTU 3 is closely related to uncultured *Isochrysis* sp. Hap7 and Hap9 from the Black Sea during early sapropel deposition around 7140–6090 BP and 5950 BP (Coolen et al., 2009), and *Isochrysis galbana* whose optimal salinity range is around 15 ppt (strain Iso; Brand, 1984). Though the salinity of North Killeak Lake is significantly lower than this range (Supplementary Table S2), it is the most saline lake among the three maar lakes, which may explain why North Killeak exhibits the highest alkenone producer diversity among the three maar lakes. Group II alkenones have been detected in a brackish lake (3.3 ppt) in

northern Alaska near the coast (Longo et al., 2016) showing that proximity to the ocean might be a source of higher salinity and Group II Isochrysidales in the lake.

4.3. Air temperature calibrations

U^K_{37} temperature calibrations in freshwater lacustrine environments with Group I Isochrysidales have shown the strongest correlation with the MTSI (Longo et al., 2018). The regressions between $U^K_{37}$and different temperatures shown in Fig. 4 suggest this index is most correlated with MTSI. This is in agreement with previous studies of water-column filtrates from Lake George (Toney et al., 2010) and sediment trap experiment from two dimictic freshwater lakes in northern Alaska (Longo et al., 2018), which shows that alkenones are produced in the water column in early spring, shortly after ice off. The regression of U^K_{37} with MTSI in this study produces a slope that is within the range of slopes in previous Group I calibrations (0.021–0.030; Zink et al., 2001; D'Andrea et al., 2011, 2016; Longo et al., 2016, 2018). Thus, using U^K_{37}-MTSI instead of U^K_{37}-MAAT may circumvent seasonal bias and provide a season-specific temperature reconstruction, and this compilation of Northern Hemisphere freshwater U^K_{37}-temperature calibrations would provide a good reference for paleotemperature reconstruction in freshwater systems.

The slight differences of U^K_{37} values in our three studied lakes might be explained by the following reasons: (1) the alkenones are extracted from a mixture of a few centimeters of sediment from the Ekman dredge, and the sedimentation rate is probably very different in the three lakes thus representing different duration of accumulation; (2) the surface area, bathymetry, and water volume of the lakes are different, which could drive spatial differences in the lake thermal regime resulting in different water temperature during the spring transition season.

4.4. Group I alkenones characteristics and RIK_{37} values

All three maar lakes investigated show a dominant $C_{37:4}$ (>40% among C_{37} alkenones) feature (White Fish: 42.5%, Devil Mountain: 48.4%, North Killeak: 60.7%) which coincides with the Group I alkenones detected in freshwater systems in Greenland (D'Andrea et al., 2006; Theroux et al., 2010), Alaska (Longo et al., 2016), Canada (Plancq et al., 2018a), and Japan (Plancq et al., 2018b).

The alkenone profiles in the maar lakes also showed significant $C_{37:3b}$ concentration. In contrast to the complicated $\%C_{37:4}$ value which can't be used alone to determine either alkenone producers or salinity, the RIK_{37} value showed more potential in identifying the alkenone producers. This index was first defined by Longo et al. (2016) as the ratio of isomeric ketones, $RIK_{37} = C_{37:3a}/(C_{37:3a} + C_{37:3b})$. Group I have a RIK_{37} value of 0.44–0.60 (Longo et al., 2016; Plancq et al., 2018a), while Group II and III have a RIK_{37} value of 1; mixed source alkenones would have a RIK_{37} value in the range 0.60–1.0. The Espenberg maar lakes all showed RIK_{37} values within the range of pure Group I alkenones (Supplementary Table S1). RIK_{37} is not able to detect Group II mixing in North Killeak. However, the number of Group II sequences recovered from the North Killeak is much lower than Group I sequences (only 3.3% of the total sequences) and this ratio might partly reflect the actual biomass, and it is possible that the Group II Isochrysidales only have minor contributions to the alkenones in this lake.

5. Conclusions

Our discovery of abundant Group I alkenones in three maar lakes on the Seward Peninsula, Alaska provides exciting new opportunities for quantitative paleotemperature reconstructions for this climatically, ecologically and anthropologically important region. Our findings highlight the presence of alkenones with clear Group I signatures in the maar lakes, together with their producers clustered into the same OTU with the sequences from Toolik Lake which are closely related to other Group I Isochrysidales discovered in BrayaSø, Greenland. The findings suggest that maar lakes with elevated pH and alkalinity are habitable for Group I Isochrysidales and U^K_{37} in these lakes are potentially powerful proxies for MTSI.

Declaration of Competing Interest

None.

Acknowledgments

This project was supported by the United States National Science Foundation awards to Y.H. (EAR-1122749, PLR-1503846, EAR-1502455; EAR-1762431), and in part by a grant from the NPS Shared Beringia Heritage program, the NPS Arctic Inventory and Monitoring Network, and NPS Bering Land Bridge National Preserve. The authors thank Scott Amy of Skydance Aviation who provides aviation and logistical support for the field samplings and Ben Meyer from University of Alaska Fairbanks for the assistance in sample collection. We are grateful for the comments from the anonymous reviewers, and editors Dr. John Volkman and Dr. Ann Pearson that helped to improve the manuscript.

Appendix A. Supplementary material

Supplementary data to this article can be found online at https://doi.org/10.1016/j.orggeochem.2019.103924.

Associate Editor—**Ann Pearson**

References

Aiken, G.R., 1992. Chloride interference in the analysis of dissolved organic carbon by the wet oxidation method. Environmental Science and Technology 26, 2435–2439.

Aponte, J.C., Dillon, J.T., Huang, Y., 2013. The unique liquid chromatographic properties of Group II transition metals for the separation of unsaturated organic compounds. Journal of Separation Science 36, 2563–2570.

Bartlein, P.J., Harrison, S.P., Brewer, S., Connor, S., Davis, B.A.S., Gajewski, K., Guiot, J., Harrison-Prentice, T.I., Henderson, A., Peyron, O., Prentice, I.C., 2011. Pollen-based continental climate reconstructions at 6 and 21 ka: a global synthesis. Climate Dynamics 37, 775–802.

Begét, J.E., Hopkins, D.M., Charron, S.D., 1996. The largest known maars on Earth, Seward Peninsula, northwest Alaska. Arctic 49, 62–69.

Brady, E.C., Otto-Bliesner, B.L., Kay, J.E., Rosenbloom, N., 2013. Sensitivity to glacial forcing in the CCSM4. Journal of Climate 26, 1901–1925.

Brand, L.E., 1984. The salinity tolerance of forty-six marine phytoplankton isolates. Estuarine, Coastal and Shelf Science 18, 543–556.

Caporaso, J.G., Bittinger, K., Bushman, F.D., DeSantis, T.Z., Andersen, G.L., Knight, R., 2009. PyNAST: a flexible tool for aligning sequences to a template alignment. Bioinformatics 26, 266–267.

Caporaso, J.G., Kuczynski, J., Stombaugh, J., Bittinger, K., Bushman, F.D., Costello, E.K., Fierer, N., Pena, A.G., Goodrich, J.K., Gordon, J.I., Huttley, G.A., 2010. QIIME allows analysis of high-throughput community sequencing data. Nature Methods 7, 335–336.

Chapin III, F.S., Trainor, S.F., Cochran, P., Huntington, H., Markon, C., McCammon, M., McGuire, A.D., Serreze, M., 2014. Alaska. In: Melillo, J.M., Richmond, T.T., Yohe, G. (Eds.), Climate Change Impacts in the United States. U.S. Global Change Research Program, pp. 514–536.

Coolen, M.J., Muyzer, G., Rijpstra, W.I.C., Schouten, S., Volkman, J.K., Sinninghe Damsté, J.S., 2004. Combined DNA and lipid analyses of sediments reveal changes in Holocene haptophyte and diatom populations in an Antarctic lake. Earth and Planetary Science Letters 223, 225–239.

Coolen, M.J., Saenz, J.P., Giosan, L., Trowbridge, N.Y., Dimitrov, P., Dimitrov, D., Eglinton, T.I., 2009. DNA and lipid molecular stratigraphic records of haptophyte succession in the Black Sea during the Holocene. Earth and Planetary Science Letters 284, 610–621.

Crump, B.C., Amaral-Zettler, L.A., Kling, G.W., 2012. Microbial diversity in arctic freshwaters is structured by inoculation of microbes from soils. The ISME Journal 6, 1629–1639.
D'Andrea, W.J., Huang, Y., 2005. Long chain alkenones in Greenland lake sediments: low $\delta^{13}C$ values and exceptional abundance. Organic Geochemistry 36, 1234–1241.
D'Andrea, W.J., Lage, M., Martiny, J.B., Laatsch, A.D., Amaral-Zettler, L.A., Sogin, M.L., Huang, Y., 2006. Alkenone producers inferred from well-preserved 18S rDNA in Greenland lake sediments. Journal of Geophysical Research: Biogeosciences 111, G03013. https://doi.org/10.1029/2005JG000121.
D'Andrea, W.J., Huang, Y., Fritz, S.C., Anderson, N.J., 2011. Abrupt Holocene climate change as an important factor for human migration in West Greenland. Proceedings of the National Academy of Sciences 108, 9765–9769.
D'Andrea, W.J., Theroux, S., Bradley, R.S., Huang, X., 2016. Does phylogeny control U37K-temperature sensitivity? Implications for lacustrine alkenone paleothermometry. Geochimica et Cosmochimica Acta 175, 168–180.
Drake, T.W., Holmes, R.M., Zhulidov, A.V., Gurtovaya, T., Raymond, P.A., McClelland, J.W., Spencer, R.G., 2019. Multidecadal climate-induced changes in Arctic tundra lake geochemistry and geomorphology. Limnology and Oceanography 64, S179–S191.
Edgar, R.C., 2010. Search and clustering orders of magnitude faster than BLAST. Bioinformatics 26, 2460–2461.
Gilbert, M.T.P., Jenkins, D.L., Götherstrom, A., Naveran, N., Sanchez, J.J., Hofreiter, M., Thomsen, P.F., Binladen, J., Higham, T.F., Yohe, R.M., Parr, R., 2008. DNA from pre-Clovis human coprolites in Oregon, North America. Science 320, 786–789.
Giordano, M., Prioretti, L., 2015. Sulphur and algae: metabolism, ecology and evolution. In: Borowitzka, M.A., Beardall, J., Raven, J.A. (Eds.), The Physiology of Microalgae. Springer, Dordrecht, The Netherlands, pp. 185–209.
Goebel, T., Waters, M.R., O'Rourke, D.H., 2008. The late Pleistocene dispersal of modern humans in the Americas. Science 319, 1497–1502.
Gran-Stadniczeñko, S., Šupraha, L., Egge, E.D., Edvardsen, B., 2017. Haptophyte diversity and vertical distribution explored by 18S and 28S ribosomal RNA gene metabarcoding and scanning electron microscopy. Journal of Eukaryotic Microbiology 64, 514–532.
Haas, B.J., Gevers, D., Earl, A.M., Feldgarden, M., Ward, D.V., Giannoukos, G., Ciulla, D., Tabbaa, D., Highlander, S.K., Sodergren, E., Methé, B., 2011. Chimeric 16S rRNA sequence formation and detection in Sanger and 454-pyrosequenced PCR amplicons. Genome Research 21, 494–504.
Hijmans, R.J., Cameron, S.E., Parra, J.L., Jones, P.G., Jarvis, A., 2005. Very high resolution interpolated climate surfaces for global land areas. International Journal of Climatology: A Journal of the Royal Meteorological Society 25, 1965–1978.
Hoffecker, J.F., Elias, S.A., O'Rourke, D.H., Scott, G.R., Bigelow, N.H., 2016. Beringia and the global dispersal of modern humans. Evolutionary Anthropology: Issues, News, and Reviews 25, 64–78.
Hopkins, D.M., 1988. The Espenberg Maars; a Record of Explosive Volcanic Activity in the Devil Mountain-Cape Espenberg Area, Seward Peninsula, Alaska. National Park Service, Alaska Regional Office.
Huelsenbeck, J.P., Crandall, K.A., 1997. Phylogeny estimation and hypothesis testing using maximum likelihood. Annual Review of Ecology, Evolution, and Systematics 28, 437–466.
Hugelius, G., Strauss, J., Zubrzycki, S., Harden, J.W., Schuur, E.A.G., Ping, C.L., Schirrmeister, L., Grosse, G., Michaelson, G.J., Koven, C.D., O'Donnell, J.A., 2014. Estimated stocks of circumpolar permafrost carbon with quantified uncertainty ranges and identified data gaps. Biogeosciences 11, 6573–6593.
Knebel, H.J., Creager, J.S., Echols, R.J., 1974. Holocene sedimentary framework, east-central Bering Sea continental shelf. In: Herman, Y. (Ed.), Marine Geology and Oceanography of the Arctic Seas. Springer, Berlin, Heidelberg, pp. 157–172.
Kurek, J., Cwynar, L.C., 2009. Effects of within-lake gradients on the distribution of fossil chironomids from maar lakes in western Alaska: implications for environmental reconstructions. Hydrobiologia 623, 37–52.
Larsen, A.S., O'Donnell, J.A., Schmidt, J.H., Kristenson, H.J., Swanson, D.K., 2017. Physical and chemical characteristics of lakes across heterogeneous landscapes in arctic and subarctic Alaska. Journal of Geophysical Research: Biogeosciences 122, 989–1008.
Longo, W.M., Dillon, J.T., Tarozo, R., Salacup, J.M., Huang, Y., 2013. Unprecedented separation of long chain alkenones from gas chromatography with a poly (trifluoropropylmethylsiloxane) stationary phase. Organic Geochemistry 65, 94–102.
Longo, W.M., Theroux, S., Giblin, A.E., Zheng, Y., Dillon, J.T., Huang, Y., 2016. Temperature calibration and phylogenetically distinct distributions for freshwater alkenones: evidence from northern Alaskan lakes. Geochimica et Cosmochimica Acta 180, 177–196.
Longo, W.M., Huang, Y., Yao, Y., Zhao, J., Giblin, A.E., Wang, X., Zech, R., Haberzettl, T., Jardillier, L., Toney, J., Liu, Z., 2018. Widespread occurrence of distinct alkenones from Group I haptophytes in freshwater lakes: implications for paleotemperature and paleoenvironmental reconstructions. Earth and Planetary Science Letters 492, 239–250.
Luecke, C., Giblin, A.E., Bettez, N.D., Burkart, G.A., Crump, B.C., Evans, M.A., Gettel, G., MacIntyre, S., O'Brien, W.J., Rublee, P.A., Kling, G.W., 2014. The response of lakes near the Arctic LTER to environmental change. In: Hobbie, J.E., Kling, G.W. (Eds.), Alaska's Changing Arctic: Ecological Consequences for Tundra, Streams, and Lakes. Oxford University Press, pp. 238–286.
Miller, G.H., Brigham-Grette, J., Alley, R.B., Anderson, L., Bauch, H.A., Douglas, M.S.V., Edwards, M.E., Elias, S.A., Finney, B.P., Fitzpatrick, J.J., Funder, S.V., 2010. Temperature and precipitation history of the Arctic. Quaternary Science Reviews 29, 1679–1715.
Moreno-Mayar, J.V., Potter, B.A., Vinner, L., Steinrücken, M., Rasmussen, S., Terhorst, J., Kamm, J.A., Albrechtsen, A., Malaspinas, A.S., Sikora, M., Reuther, J.D., 2018. Terminal Pleistocene Alaskan genome reveals first founding population of Native Americans. Nature 553, 203–207.
O'Donnell, J.A., Aiken, G.R., Butler, K.D., Douglas, T.A., 2015. Chemical composition of large lakes in Alaska's Arctic Network: 2013–2014. Natural Resource Data Series NPS/ARCN/NRDS 2015/985. National Park Service, Fort Collins, Colorado.
O'Donnell, J.A., Aiken, G.R., Swanson, D.K., Panda, S., Butler, K.D., Baltensperger, A.P., 2016. Dissolved organic matter composition of Arctic rivers: linking permafrost and parent material to riverine carbon. Global Biogeochemical Cycles 30, 1811–1826.
Pecoraino, G., D'Alessandro, W., Inguaggiato, S., 2015. The other side of the coin: geochemistry of alkaline lakes in volcanic areas. In: Volcanic Lakes. Springer, Berlin, Heidelberg, pp. 219–237.
Plancq, J., Cavazzin, B., Juggins, S., Haig, H.A., Leavitt, P.R., Toney, J.L., 2018a. Assessing environmental controls on the distribution of long-chain alkenones in the Canadian Prairies. Organic Geochemistry 117, 43–55.
Plancq, J., McColl, J.L., Bendle, J.A., Seki, O., Couto, J.M., Henderson, A.C., Yamashita, Y., Kawamura, K., Toney, J.L., 2018b. Genomic identification of the long-chain alkenone producer in freshwater Lake Toyoni, Japan: implications for temperature reconstructions. Organic Geochemistry 125, 189–195.
Richter, N., Longo, W.M., George, S., Shipunova, A., Huang, Y., Amaral-Zettler, L., 2019. Phylogenetic diversity in freshwater-dwelling Isochrysidales haptophytes with implications for alkenone production. Geobiology 17, 272–280.
Schuur, E.A., McGuire, A.D., Schädel, C., Grosse, G., Harden, J.W., Hayes, D.J., Hugelius, G., Koven, C.D., Kuhry, P., Lawrence, D.M., Natali, S.M., 2015. Climate change and the permafrost carbon feedback. Nature 520, 171–179.
Simon, M., López-García, P., Moreira, D., Jardillier, L., 2013. New haptophyte lineages and multiple independent colonizations of freshwater ecosystems. Environmental Microbiology Reports 5, 322–332.
Stamatakis, A., 2014. RaxML version 8: a tool for phylogenetic analysis and post-analysis of large phylogenies. Bioinformatics 30, 1312–1313.
Takahashi, H., Kopriva, S., Giordano, M., Saito, K., Hell, R., 2011. Sulfur assimilation in photosynthetic organisms: Molecular functions and regulations of transporters and assimilatory enzymes. Annual Review of Plant Biology 62, 157–184.
Tamm, E., Kivisild, T., Reidla, M., Metspalu, M., Smith, D.G., Mulligan, C.J., Bravi, C.M., Rickards, O., Martinez-Labarga, C., Khusnutdinova, E.K., Fedorova, S.A., 2007. Beringian standstill and spread of Native American founders. PloS One 2, e829.
Theroux, S., D'Andrea, W.J., Toney, J., Amaral-Zettler, L., Huang, Y., 2010. Phylogenetic diversity and evolutionary relatedness of alkenone-producing haptophyte algae in lakes: implications for continental paleotemperature reconstructions. Earth and Planetary Science Letters 300, 311–320.
Toney, J.L., Huang, Y., Fritz, S.C., Baker, P.A., Grimm, E., Nyren, P., 2010. Climatic and environmental controls on the occurrence and distributions of long chain alkenones in lakes of the interior United States. Geochimica et Cosmochimica Acta 74, 1563–1578.
Vachula, R.S., Huang, Y., Longo, W.M., Dee, S.G., Daniels, W.C., Russell, J.M., 2019. Evidence of Ice Age humans in eastern Beringia suggests early migration to North America. Quaternary Science Reviews 205, 35–44.
Wang, L., Longo, W.M., Dillon, J.T., Zhao, J., Zheng, Y., Moros, M., Huang, Y., 2019. An efficient approach to eliminate steryl ethers and miscellaneous esters/ketones for gas chromatographic analysis of alkenones and alkenoates. Journal of Chromatography A 1596, 175–182.
Weishaar, J.L., Aiken, G.R., Bergamaschi, B.A., Fram, M.S., Fujii, R., Mopper, K., 2003. Evaluation of specific ultraviolet absorbance as an indicator of the chemical composition and reactivity of dissolved organic carbon. Environmental Science and Technology 37, 4702–4708.
Zheng, Y., Tarozo, R., Huang, Y., 2017. Optimizing chromatographic resolution for simultaneous quantification of long chain alkenones, alkenoates and their double bond positional isomers. Organic Geochemistry 111, 136–143.
Zink, K.G., Leythaeuser, D., Melkonian, M., Schwark, L., 2001. Temperature dependency of long-chain alkenone distributions in recent to fossil limnic sediments and in lake waters. Geochimica et Cosmochimica Acta 65, 253–265.